Dalton Transactions

Accepted Manuscript

This is an *Accepted Manuscript*, which has been through the Royal Society of Chemistry peer review process and has been accepted for publication.

Accepted Manuscripts are published online shortly after acceptance, before technical editing, formatting and proof reading. Using this free service, authors can make their results available to the community, in citable form, before we publish the edited article. We will replace this *Accepted Manuscript* with the edited and formatted *Advance Article* as soon as it is available.

You can find more information about *Accepted Manuscripts* in the Information for Authors.

ROYAL SOCIETY OF CHEMISTRY

www.rsc.org/dalton

Cite this: DOI: 10.1039/c0xx00000x

www.rsc.org/xxxxxx ARTICLE TYPE

In-situ spectroscopic study of the local structure of oxyfluoride melts: NMR insight into the speciation in molten LiF-LaF_3-Li_2O systems

Anne-Laure Rollet,*[a,b] Haruaki Matsuura[c,b] and Catherine Bessada[b]

Received (in XXX, XXX) Xth XXXXXXXXX 20XX, Accepted Xth XXXXXXXXX 20XX
DOI: 10.1039/b000000x

The local structure of molten LaF_3-LiF-Li_2O has been investigated using High Temperature NMR spectroscopy. The ^{139}La and ^{19}F chemical shifts have been measured as a function of temperature and composition. The NMR spectra show that Li_2O reacts completely with LaF_3 to form LaOF compound at the solid state below the melting temperature of the sample. LaOF is not completely dissolved in the fluoride melt and solid LaOF is observed on the ^{19}F spectra for Li_2O concentration above 10mol%. We discuss the local environment of lanthanum ions in molten LaF_3-LiF-Li_2O and compared the results to those with LaF_3-LiF-CaO system. The analysis of the temperature and Li_2O concentration dependences of the ^{139}La and ^{19}F chemical shifts suggests that several kinds of lanthanum oxyfluoride long-lived $LaO_xF_y^{3-x-y}$ units are present in the melt.

1. Introduction

The description of the oxyfluoride structure at the liquid state is at its very first step. The oxyfluorides are the evident bridge between the oxides and the fluorides fields. Nevertheless, the researches use to be focused in only one or the other domain because their respective experimental requirements are really different and very severe (high temperature, corrosiveness, volatility…). As an example, the cell material for spectroscopic investigation suitable for oxides (other oxide like alumina) are dissolved by molten fluorides and reversely boron nitride used for fluorides reacts with molten oxides. These factors have lead to separate these two domains of research and to leave the oxyfluorides not studied relatively.

The local structure in molten salts is often discussed in terms of coordination numbers, radial distribution functions and possible 'complex' species which lifetime is typically around the picosecond.[1,2,3] In molten fluorides, such information has been experimentally brought by Raman[4,5,6], NMR[7,8,9,10] and EXAFS[11,12,13,14] spectroscopies. Molten fluorides are particularly interesting systems because their liquid structure may switch from a simple bath of charged hard spheres to a loose ionic network or a liquid with free 'complexes'.[1,15] Typically, molten LaF_3-LiF structure spans with the LaF_3 molar fraction (x_{LaF3}) from free LaF_x^{3-x} units (x_{LaF3}<0.1) to loose ionic network (x_{LaF3}>0.2).[16] It turns out that the lifetime of these configurations is crucial for the physical and chemical properties of the melt.[2] In molten oxides, Raman,[17,18,19] and NMR[20,21] spectroscopies have been also employed but mainly X-Ray[22,23] and neutron scattering.[24,25] Similarly to fluorides, oxides exhibit various liquid structures that span from ionic liquids to glasses with covalent bonds.[26] The understanding of both molten fluorides and oxides has taken great benefit from the advances brought by Madden and his co-workers in numerical simulations.[27,28] They described successfully both the molten fluorides[29,30,31] and oxides,[32,33,34]. They are able to well reproduce experimental EXAFS[35] and Raman[36] data testifying hence of their reliablity. Combined to experiments they gave a new impact to molten salts understanding. Despite all these works on molten salts, no experimental or numerical study has been devoted to the local description of oxyfluoride melts yet. Only few papers have studied the effect of small amount of oxide on the structure of molten fluorides.[37,38,39,9]

In this paper, we investigate the molten LaF_3-LiF-Li_2O system. Lanthanum typifies the large rare earths that are nowadays utilized in most advanced technology. Their polluting production procedure and their exportation is even a source of political and econimal tension between countries.[40] Rare earth recycling thus becomes an important issue. For rather different reasons, rare earth recycling is also crucial in the nuclear engineering field: they are wastes produced by the nuclear reactions. In molten salt nuclear reactor (MSR), they have to be removed continously from the liquid fuel because they are poison to the nuclear reaction.[41] In more traditionnal nuclear reactor (with a solid fuel), rare earth extraction has to be performed by considering either their radioactive period for geological storage or their ability to be burnt. For all these recycling needs, the molten salts processes appear to be a good candidate.[42, 43, 44]

In order to describe the local structure of molten LaF_3-LiF-Li_2O sytem, we use high temperature nuclear magnetic resonance spectroscopy (HT NMR). This technique gives insight into the first shells around ^{139}La, ^{19}F and into the potential network formation via bridging fluorine and oxygen.

2. Experimental and methods

All reagents used for experiments (LaF_3, LiF and Li_2O, purity 99.99%) were purchased from Alfa Aesar. The appropriate

quantities of binary mixtures were weighed and then put into NMR crucibles in a glove box under dried Argon atmosphere in order to avoid H_2O and O_2 contamination of the samples. The NMR crucibles are made in boron nitride (BN) without oxide binder and are tightly closed by a screwed cap also in BN. The amount of salt in each crucible is ca. 100 mg.

The High Temperature NMR (HT NMR) spectra were recorded using a Bruker Avance WB 400MHz spectrometer, operating at 9.40 T. *In situ* HT NMR spectra were obtained by using the CO_2 laser heating system developed at CEMHTI-CNRS in Orléans, France[45]. In this study, the samples are heated by 2 lasers that irradiate the top and the bottom of the sample in order to reduce the temperature gradient. The temperature cannot be measured *in situ* during the measurement but is calibrated using a series of reference compounds. Some of the salts were checked before and after the HT NMR experiments using X-ray diffraction (Bruker D8 diffractometer).

The HT NMR spectra were acquired using a single pulse sequence, with a recycle delay of 0.5 s, and 8 to 128 accumulations. The pulses were $\pi/2$ for ^{19}F and ^{139}La HT NMR.

The chemical shifts were referred to CCl_3F for ^{19}F and $LaCl_3$ 1M aqueous solution for ^{139}La. All NMR spectra have been treated by the dmfit program[46].

3. Results and discussion

The effect of increasing amount of Li_2O in molten LaF_3-LiF has been firstly and more extensively studied for the LaF_3-LiF 20-80 mol% composition (noted $LaLi_4F_7$ in the following for convenience although there is no such define solid compound) in section 3.1 and 3.2. The effect of the amount of Li^+ ions compared with La^{3+} ions has been also investigated in section 3.3 with LaF_3-LiF 10-90 mol% and 30-70 mol% compositions.

To help the discussion the chemical shift values of key compositions measured in this work are gathered in Table 1.

Table 1: Chemical shifts of key compounds (ppm)

	^{19}F			^{139}La	
compound	**RT solid**	**HT solid**	**Liquid**	**RT solid**	**Liquid**
LiF	-201	-201	-201	-	-
LaF_3	-25.2, 12.4 and 19.7 Weighted average =-8	+10	+52	-129	-60
LaF_3-LiF (x_{LaF3}=0.2)	*	*	-90	*	-51
LaOF	-35	-10			

* As there is no defined phase of solid compound at this composition, so the chemical shifts of ^{19}F and ^{139}La are those of pure LaF_3 and LiF.

LiF has a CFC crystal structure that is kept upto the liquid; in the liquid, the average coordination number of both ions is about 4.[47,48] LaF_3 crystallizes at room temperature in P -3 c 1 space group where lanthanum occupies one site surrounded by 9 fluorine and fluorine occupies 3 sites (F1, F2, F3) surrounded by 3 lanthanum and 3 fluorine for F1 and F2 and by 3 lanthanum for F3.[49,50,51] LaOF crystallizes at room temperature in P 4/n m m space group[52] where lanthanum is surrounded by 4 fluorine and 4 oxygen and both the fluorine and the oxygen are surrounded by 4 lanthanum. LaOF follows a phase transition at 778K,[53] its space group is then F m -3 m where lanthanum is still surrounded by 8 anions nevertheless oxygen and fluorine share the same site.[54] Hence there is 24 possible configurations around lanthanum. The coordination number of fluorine is equal to the one in LaOF at room temperature but the fluorine-lanthanum distance is longer.

The characterization of the samples after the NMR experiments is displayed in the ESI (Figures S1 and S2). The important point is that whatever the ratio O/La investigated here (from x_{Li2O} = 0 to 0.5) the whole Li_2O has reacted with LaF_3 to form LaOF and no La_2O_3 was observed.

3.1. Behaviour during heating and temperature dependence

In this section, we present the evolution of the NMR spectra versus temperature from room temperature upto 100-200 K above the melting point. Several procedures of heating have been used: (1) progressive heating from room temperature and (2) heating directly up to the liquidus temperature. The goal is to evidence the melting behaviour and / or the signature of reaction with oxide in solid. Indeed, it appeared during the first experiments that the dissolution was not a simple process. Moreover, LaOF can be formed by mecanosynthesis with LaF_3 and Li_2O.[55,56]

Figures 1a and 1b show the NMR spectra of ^{19}F and ^{139}La from 700K to 1290 K in $LaLi_4F_7$ + Li_2O (x_{Li2O} = 0.2) and in ESI are presented the similar figures for $LaLi_4F_7$ without Li_2O, with Li_2O (x_{Li2O} = 0.1, 0.3 and 0.5).

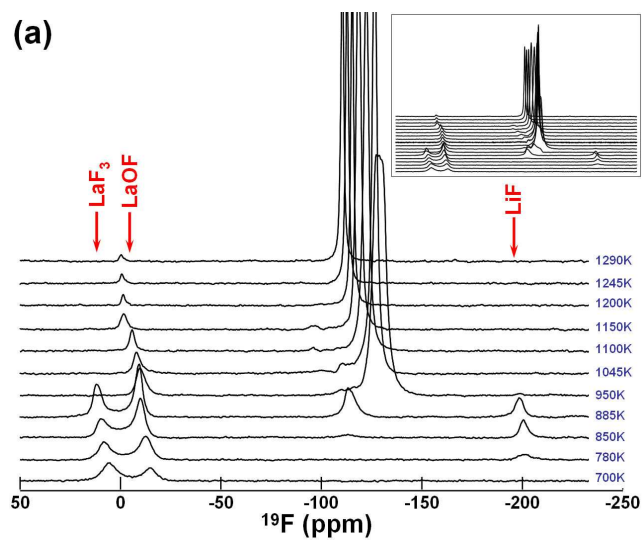

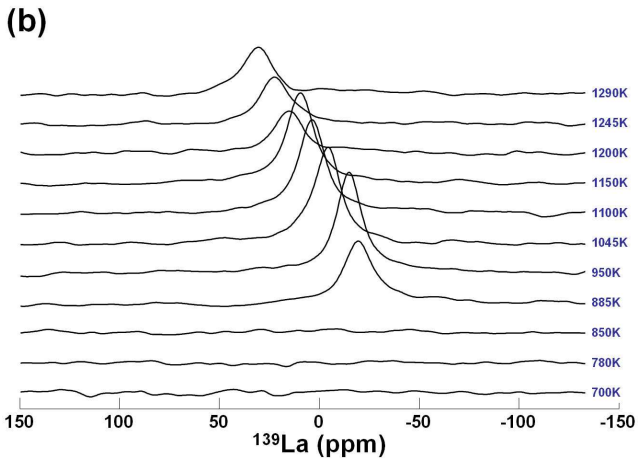

Fig.1. ^{19}F (a) and ^{139}La (b) NMR spectra of $LaLi_4F_7$ + Li_2O (x_{Li2O} = 0.20) for increasing temperature. For ^{19}F spectra, the liquid peak (-120ppm) is cut in order to make it possible to see the secondary peaks, in the inlet the full spectra are plotted.

^{19}F. Before discussing the results presented in Figure 1a, it is important to recall that the observation characteristic time of NMR spectroscopy does not make it possible to observe the different 'complexes' present in the melt. The nucleus experiences all the different environments during the measurement and NMR spectrum is made of only one sharp peak. Nevertheless, this peak is the weighted average of all the individual peak positions that should be if the measurement was infinitely fast. On the contrary, the NMR spectrum of a solid yields to as many peaks as there are different environments for the observed nucleus provided the resolution is sufficient. In the ^{19}F NMR spectra presented in Figure 1a, two peaks are already visible at 700 K. At this temperature the sample is still at the solid state as determined by complementary DSC experiments. The peak around +10 ppm corresponds to LaF_3 solid as illustrated in Figure 2 where the ^{19}F spectra of pure polycrystalline LaF_3 at 775 K is displayed.

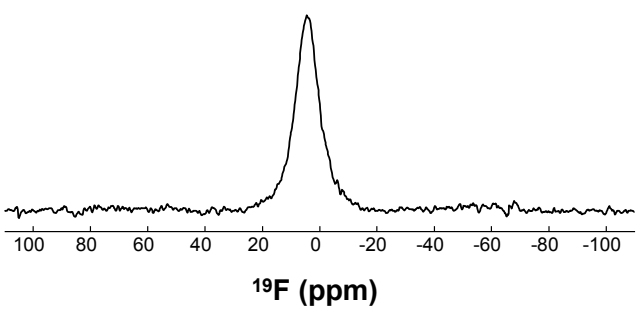

Fig.2. ^{19}F NMR spectra of pure LaF_3 recorded using a HT static probe at 775K.

On the figure 1a, the position of LaF_3 peak is shifted toward positive value by increasing temperature. The peak around -10 ppm is attributed to LaOF solid. Its position is also shifted toward positive value by increasing the temperature. Hence, Li_2O and LaF_3 rapidly react at the solid state to form LaOF. The solid state reaction has been also evidenced in the $LaLi_4F_7$+CaO system.[57] At 700K, only one peak is observed for LaF_3. Previous NMR studies on monocrystalline and polycrystalline LaF_3 have shown that the fluorine are in rapid exchange between the 3 crystallographic sites at this temperature.[58,59] One peak is observed for LaOF as expected from its crystallographic structure. The fluorines of LiF cannot be observed at 700K contrary to those of LaF_3 and LaOF because the mobility of its fluorine ions is much less. LaF_3 and LaOF are good ionic conductor with fluorine as conducting species (LaF_3 [60,61,62,63,64] being however a much better ionic conductor than LaOF [65,66]). These peaks are shifted toward positive chemical shift values with temperature (see also ESI). The characteristic peak of LiF (-201ppm) appears around 850K. In the same time, the intensity of LaOF peak increases contrary to the one of LaF_3 that decreases. Around 950K a new peak appears around -110ppm along with a very broad peak in the ^{139}La spectrum. This ^{19}F peak is the first sign of the liquid appearance. At 1050K, the sample is liquid and both the LiF and LaF_3 peaks have disappeared. The LaOF peak remains even at the highest temperature investigated here (1300K). As explained in the introduction of this section, the observation of a secondary peak while the salt is molten indicates that either a solid compound remains in the sample or the sample is multiphasic. It means that LaOF is not completely dissolved in the LaF_3-LiF melt. The LaOF peak appears around 10mol% Li_2O. This value is in agreement with the one observed in the $LaLi_4F_7$+CaO system (around 13mol% CaO). It is also in agreement with the solubility of LaOF determined in LiF-NaF and in LaF_3-LiF melts.[67,57] Its solubility constant is indeed relatively low and is about 10^{-3} in molten $LaLi_4F_7$ at 1115K and in LiF-NaF at 1075K.

The peak of the liquid (-147ppm) is shifted toward positive values with increasing temperature and becomes thinner. The full width at half maximum (FWHM) of the ^{19}F NMR peak is correlated to the viscosity and by increasing the temperature the latter decreases. In the same time, the LaOF peak intensity decreases (and is also shifted toward positive values): it means that the amount the dissolved LaOF increases with temperature as expected.

^{139}La. The ^{139}La spectra are consistent with the ^{19}F spectra: a broad peak appears around T= 890K and as for ^{19}F corresponds to the first sign of the liquid, the melting being complete at 1050K (Figure 1b). However, contrary to ^{19}F, only one peak is observed. The signature of solid LaOF cannot be observed in the ^{139}La spectra due to the NMR characteristic of this nucleus (large quadrupolar constant that makes its solid spectra very broad and unobservable using the HT NMR static probe at 9 Teslas). The ^{139}La peak is shifted toward positive chemical shift values with temperature similarly to the ^{19}F peak.

Rapid heating procedure of samples leads to the same results in the liquid as the slow heating procedure: solid LaOF remains visible upto 1300 K.

At the liquid state, the evolution of the chemical shifts of ^{19}F and ^{139}La with temperature is low in the mixture without oxide, as already observed for other molten RF_3-MF (R=rare earth and M=alkaline).[68] This evolution is stronger when oxide are added in the melt. It is similar from x_{Li2O} = 0.1 to x_{Li2O} = 0.3 and becomes much stronger above. It is difficult to deconvolute the effect of temperature on the liquid structure for a given composition (i.e. a given amount of dissolved LaOF) and the variation of dissolved LaOF amount in the melt due to the temperature. Nevertheless, this change in the temperature dependence may be connected to a

change in the $LaO_xF_y^{3-x-y}$ units present in the melt. The NMR peaks of both ^{19}F and ^{139}La appears to be larger around $x_{Li2O} = 0.3$ supporting the idea of a change in the liquid structure (Figure 3). The full width at half maximum (FWHM) gives an insight into the viscosity of the melt. The variation observed in Figure 3 may indicate that above $x_{Li2O} = 0.3$, chains of -La-O-La-O- are formed in the melt. This is similar to what has been already evidenced in molten RF_3-AF [69,70,2] and ZrF_4-AF [71,69] however the lifetime of these configurations seems to be much longer.

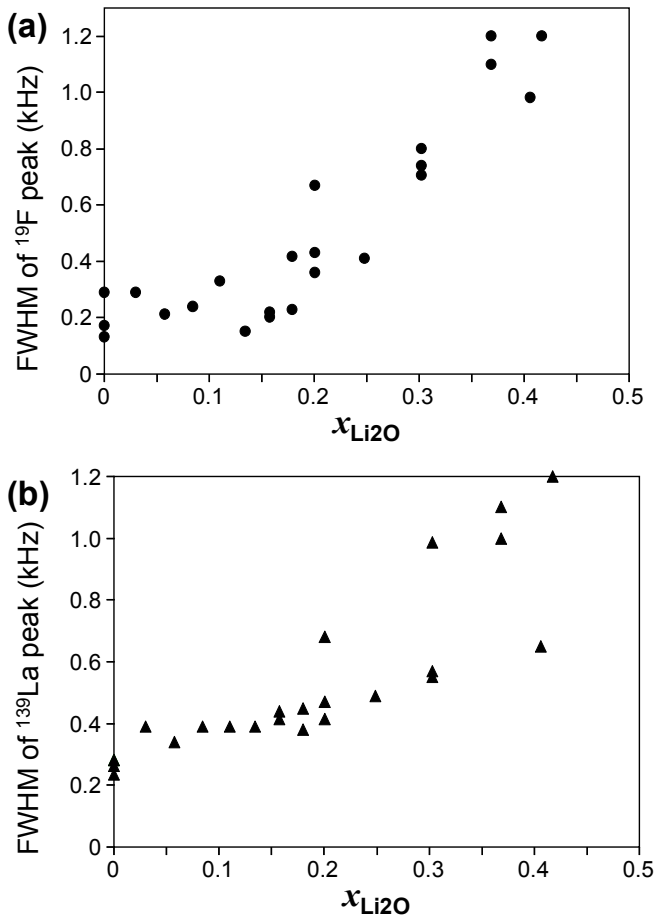

Fig.3. FWHM of the ^{19}F (a) and ^{139}La (b) NMR peaks in molten $LaLi_4F_7$ + Li_2O versus the molar fraction in Li_2O.

3.2 Oxide amount dependence

In this section on the oxide amount dependence, we restrict the discussion at the temperature 1100K. The ^{19}F and ^{139}La chemical shifts of the liquid peak are plotted as a function of the Li_2O molar fraction x_{Li2O} in Figure 4. The values for the LaF_3-LiF-CaO system extracted from ref 57 have been also plotted for comparison. With increasing oxide amount, the ^{19}F chemical shift moves toward negative values almost linearly (Figure 4a). This evolution is the same as the one observed when CaO is added to $LaLi_4F_7$; both curves superimposes each other. The displacement toward negative values indicates that the fluorine environment goes toward a "LiF" environment, i.e. that fluorine anions are removed from the first neighbour shell of La and are replaced by oxygen anions. The ^{139}La chemical shift moves toward positive values (Figure 4b). This evolution is similar to the one observed when CaO is added to $LaLi_4F_7$; however, contrary to ^{19}F both curves do not superimpose each other. With Li_2O the evolution of the ^{139}La chemical shift is much stronger than with CaO.

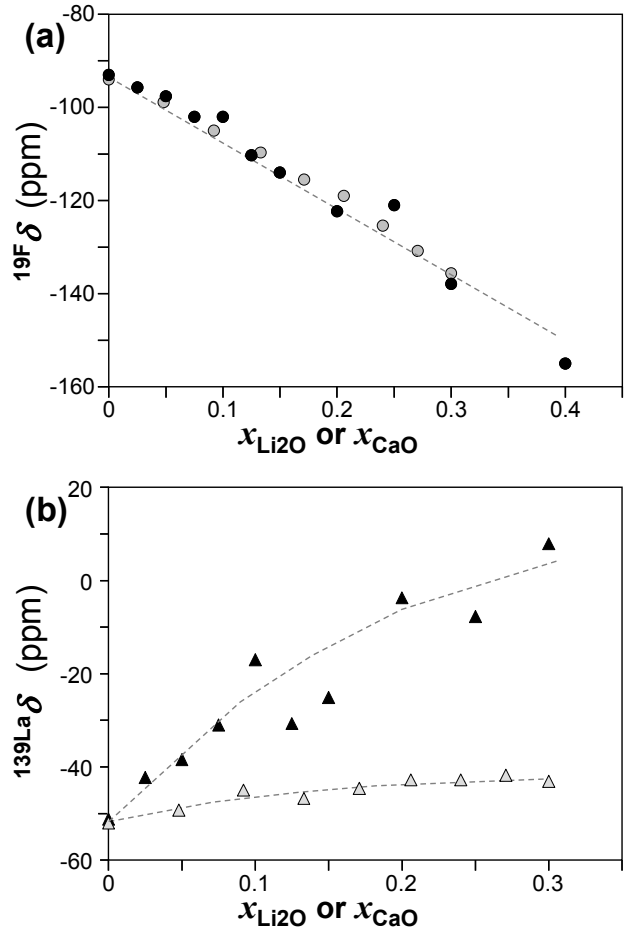

Fig.4. ^{19}F (a) and ^{139}La (b) chemical shift in molten $LaLi_4F_7$ + Li_2O versus the concentration of Li_2O (black symbol) at 1100K. For comparison the $LaLi_4F_7$ + CaO system is also plotted (grey symbol).

This difference may be attributed to the difference of fluoro-acidity between Li^+ and Ca^{2+}. Recently, a new electrochemical method to build a fluoroacidity scale has been proposed by the LGC's team in Toulouse – France based on the measurement of the equilibrium between gazeous SiF_4 or BF_3 and dissolved in molten fluorides.[72,73] They have shown that the CaF_2-LiF is more acidic than LiF, i.e. fluorine anions are less available in CaF_2-LiF than in LiF. In addition, it has been shown that Ca^{2+} cations induce less change in the La^{3+} local environment than Li^+. In molten $CaLi_4F_6$-LaF_3, La^{3+} environment appears to be almost the same as in pure molten LaF_3 while in LiF-LaF_3,[57] La^{3+} is surrounded by slightly less fluorine anions.[16] Furthermore, Ca^{2+} ions has higher affinity for O^{2-} ions than Li^+ ions.[74,75] This fact is evidenced here by the LaOF peak in the ^{19}F spectra that appears at lower oxide content for Li_2O than for CaO. It may therefore be conjectured that the long-lived lanthanum oxyfluoride $LaO_xF_y^{3-x-y}$ units are different in CaO and Li_2O addition cases with an average x greater with Li_2O than with CaO. This hypothesis is consistent with the trend of the ^{139}La isotropic chemical shift in solid compounds: it goes from –135 ppm in LaF_3 [16,76] and -60 ppm in $RbLaF_4$ [77] to + 375 ppm in $LaAlO_3$,[78] + 600 ppm in $LaGaO_3$ [79] and + 640 ppm in La_2O_3.[80] Hence,

replacing fluorine by oxygen around lanthanum induces a important displacement of the ^{139}La isotropic chemical shift toward positive values. This hypothesis is also supported by the evaluation of the ^{139}La and ^{19}F chemical shifts. In molten salts such as molten fluorides, the lifetime of each structural configuration is much shorter than the characteristic time of NMR measurement. The measured chemical shift $\delta_{measured}$ is thus the weighted average of all the individual values δ_i corresponding to all the different environments experienced by the nucleus during the time of the experiment:

$$\delta_{measured} = \sum_i a_i \delta_i \quad (1)$$

Therefore, if all the $a_i\delta_i$ can be assessed, then $\delta_{measured}$ can be calculated. Using this procedure, the ^{139}La and ^{19}F chemical shifts for the $LaLi_4F_7$-CaO system could be nicely reproduced using only one kind $LaOF_x^{3-x}$ unit. For the $LaLi_4F_7$-Li_2O system, such an approach fails and several $LaOF_x^{3-x}$ units should be considered (in this case, the constraint on the calculation of the curves of Figure 4 is insufficient to yield to valid result). Hence, the molten $LaLi_4F_7$-Li_2O system may contain both isolated $LaOF_x^{3-x}$ long-lived units and bigger units $LaO_xF_y^{3-x-y}$ which proportions change with the concentration of Li_2O. Note that longer lanthanum oxyfluoride chains can even occur.

3.3. Lithium amount dependence

In this section, we address the influence of the ratio n_{La}/n_{Li} (or n_{La}/n_F). By changing this ratio, one changes the fluoroacidity of the melt. Two other compositions from each side of the $LaLi_4F_7$ composition have been used: LaF_3-LiF 10-90mol% where $n_{La}/n_{Li} = 0.111$ and $n_{La}/n_F = 0.083$ and LaF_3-LiF 30-70mol% where $n_{La}/n_{Li} = 0.426$ and $n_{La}/n_F = 0.188$. In LaF_3-LiF 20-80mol%, $n_{La}/n_{Li} = 0.25$ and $n_{La}/n_F = 0.143$. Nevertheless, this comparison is not straightforward because the temperature could not be the same for the three system. Indeed, the liquidus of LaF_3-LiF 10-90mol% and LaF_3-LiF 20-80mol% are approximately the same, ca 1100K, but it is much higher for LaF_3-LiF 30-70mol%, ca 1250K. We therefore have chosen to run each experiment at the liquidus temperature of the corresponding LaF_3-LiF mixture without oxide. In the ESI the position of our experiments are placed in several LaF_3-LiF phase diagrams determined by different groups[81,82,83,84,85] (Figure S10).

The ^{19}F and ^{139}La chemical shifts of the liquid peak are plotted versus the ratio n_O/n_{La} in Figure 5. The variation of ^{19}F chemical shift is similar for the three ratio n_{La}/n_{Li} investigated here. The $^{19F}\delta$ value for the three systems seems to converge on ca -200ppm at n_O/n_{La}=1. Interestingly, $^{19F}\delta = -200$ ppm is the value measured in neat molten LiF. It is important here to stress that the values plotted in Figure 5a correspond to the main peak shown in Figure 1a but the LaOF remains in all the compositions rich in oxide.

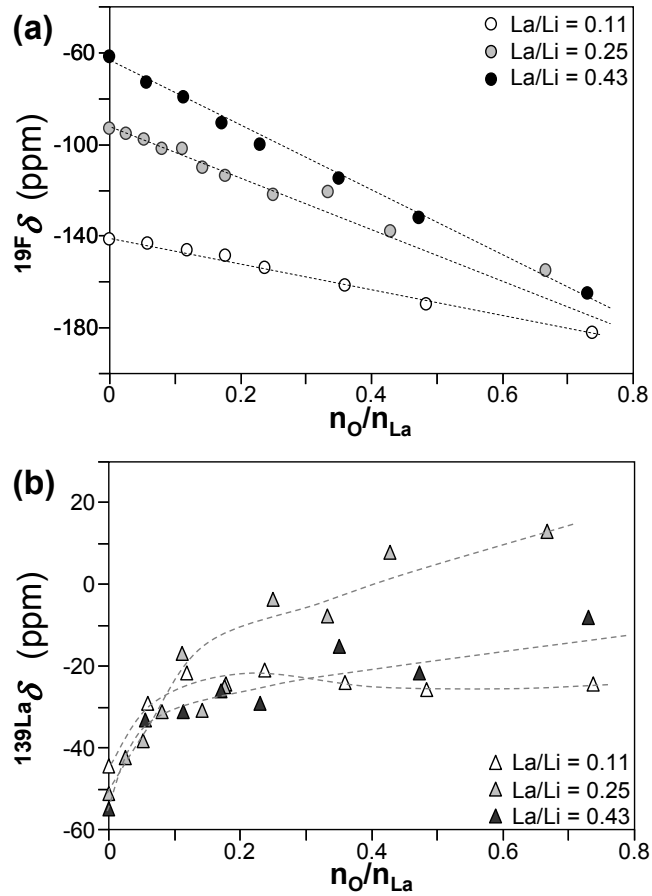

Fig.5. ^{19}F (a) and ^{139}La (b) chemical shift in molten LaF_3-LiF + Li_2O versus the ratio n_O/n_{La} for $n_{La}/n_{Li} = 0.111$ (white symbol), $n_{La}/n_{Li} = 0.25$ (grey symbol) and $n_{La}/n_{Li} = 0.426$ (black symbol) at 1100K.

The variation of ^{139}La chemical shift $^{139La}\delta$ is also similar for the three ratio n_{La}/n_{Li}: rapid increase up to n_O/n_{La} = 0.1 then slow increase or plateau. For La/Li = 0.11 a plateau is observed while a slow increase occurs for La/Li = 0.25. The comparison between La/Li = 0.11 and La/Li = 0.25 is easier as the running temperature were the same. From their curves it seems that the richer melt in lanthanum, the higher proportion O/La accessible. The more fluoroacidic melt, the higher quantity of LaOF.

Conclusions

The local structure of molten LaF_3-LiF-Li_2O system has been investigated thanks to HT NMR. By increasing the temperature from room temperature upto the liquidus temperature, Li_2O reacts at the solid state with LaF_3 to form LaOF; at the liquidus temperature of LaF_3-LiF, LaOF is dissolved in the melt. The amount of dissolved LaOF increases when temperature is increased but the solubility remains low (Ks ~ 10^{-3}). The variations of ^{19}F and ^{139}La chemical shifts in the melt indicate the formation of $LaO_xF_y^{3-x-y}$ long-lived units with possible chains of -La-O-La-O- kind.

Acknowledgements

Authors express special thanks to Emmanuel Veron for X-ray diffraction, to Sandra Ory for DSC, to Eric Labrude for machining special NMR crucibles and to Aydar Rakhmatullin for

valuable discussion (CEMHTI). We are also grateful to the JSPS and CNRS for the financial support of the Joint Project between the Japanese and French partners under the "Japan-France (JSPS-CNRS) Research Cooperative Program". HM wishes to thank the colleagues and staffs of le STUDIUM to encourage the continuation of the collaboration research both in France and Japan.

Notes and references

[a] *PHENIX - CNRS – UPMC, case 51, 4 place Jussieu, 75252 Paris cedex 05, France. Tel: 33 1 4427 3049; E-mail: anne-laure.rollet@upmc.fr*
[b] *CEMHTI - CNRS, 1D avenue de la Recherche Scientifique, 45071 Orléans Cedex 2, France. E-mail: catherine.bessada@cnrs-orleans.fr*
[c] *Research Laboratory for Nuclear Reactors, Tokyo Institute of Technology, 2-12-1-N1-10, Ookayama, Meguro-ku, Tokyo 152-8550, Japan. Tel: +81 3 5734 3076; E-mail: hmatsuur@nr.titech.ac.jp*

† Electronic Supplementary Information (ESI) available: XRD and NMR characterization of solidified samples; HT NMR ^{19}F and ^{139}La spectra of molten $LaLi_4F_7$ + Li_2O with x_{Li2O} = 0, 0.1, 0.3, 0.5; position of the HT NMR experiments in the LaF_3-LiF phase diagram. See DOI: 10.1039/b000000x/

1 A.–L. Rollet and M. Salanne, *Annu. Rep. Prog. Chem. Sect. C, Phys. Chem.*, 2011, **107**, 88.
2 M. Levesque, V. Sarou-Kanian, M. Salanne, M. Gobet, H. Groult, C. Bessada, P. A. Madden and A.-L. Rollet, *J. Chem. Phys.*, 2013, **138**, 184503.
3 S. A. Kirillov, E. A. Pavlatou and G. N. Papatheodorou, *J. Chem. Phys.*, 2002, **116**, 9341.
4 V. Dracopoulos, D. Th. Kastrissios and G. N. Papatheodorou, *J. Non-Cryst. Solids*, 2005, **351**, 640.
5 F. Auguste, O. Tkatcheva, H. Mediaas, T. Ostvold and B. Gilbert, *Inorg. Chem*., 2003, **42(20)**, 6338.
6 V. Dracopoulos, B. Gilbert and G. N. Papatheodorou, *J. Chem. Soc. Faraday Trans.*, 1998, **94(1)**, 2601.
7 C. Bessada, A.-L. Rollet, A. Rakhmatullin, I. Nuta, P. Florian and D. Massiot, *C.R. Chimie*, 2006, **9**, 374.
8 A.–L. Rollet and C. Bessada, *Annu. Rep. Prog. Chem. Sect. C, Phys. Chem.*, 2013, **78**, 149.
9 V. Lacassagne, C. Bessada, P. Florian, S. Bouvet, B. Ollivier, J.-P. Coutures and D. Massiot, *J. Phys. Chem. B*, 2002, **106**, 1862.
10 C. Bessada, A. Rakhmatullin, A.–L. Rollet and D. Zanghi, *J. Fluorine Chem*., 2009, **130**, 45
11 S. Watanabe, A.K. Adya, Y. Okamoto, N. Umesaki, T. Honma, H. Deguchi, M. Horiuchi, T. Yamamoto, S. Noguchi, K. Takase, A. Kajinami, T. Sakamoto, M. Hatcho, N. Kitamura, H. Akatsuka and H. Matsuura, *J. Alloys Compd*., 2006, **408**, 71.
12 A.-L. Rollet, C. Bessada, Y. Auger, P. Melin, M. Gailhanou and D. Thiaudière, *Nucl. Instrum. Methods Phys. Res., Sect. B*, 2004, **226**, 447.
13 H. Matsuura, S. Watanabe, H. Akatsuka, Y. Okamoto and A.K. Adya, *J. Fluorine Chem.*, 2009, **130**, 53.
14 O. Pauvert, D. Zanghi, M. Salanne, C. Simon, A. Rakhmatullin, H. Matsuura, Y. Okamoto, F. Vivet and C. Bessada, *J. Phys. Chem*., 2010, **114,** 6472.
15 M. P. Tosi, D. L. Price and M.-L. Saboungi, *Annu. Rev. Phys. Chem.*, 1993, **44**, 173.
16 A.–L. Rollet, S. Godier and C. Bessada, *Phys. Chem. Chem. Phys.*, 2008, **10**, 3222.
17 P. Simon, B. Moulin, E. Buixaderas, N. Raimboux, E. Herault, B. Chazallon, H. Cattey, N. Magneron, J. Oswalt and D. Hocrelle, *J. Raman Spectrosc.*,2003, **34**, 497.
18 A.K. Hassan, L.M. Torell, L. Borjesson and H. Doweider, *Phys. Rev. B*, 1992, 45, 12797.
19 G. N. Papatheodorou and A. G. Kalampounias, *J. Phys.: Condens. Matter*, 2009, 21, 205101.
20 D. Massiot, F. Fayon, V. Montouillout, N. Pellerin, J. Hiet, C. Roiland, P. Florian, J.-P. Coutures, L. Cormier and D. R. Neuville, *J. Non-Crystalline Solids.*, 2008, **354**, 249.
21 J.F. Stebbins and I. Farnan, *Science*, **255**, 586 (1992).
22 G. N. Greaves, M. C. Wilding, S. Fearn, D. Langstaff, F. Kargl, S. Cox,1 Q. Vu Van, O. Majérus, C. J. Benmore, R. Weber, C. M. Martin and L. Hennet, *Science*, 2008, **322** , 566.
23 L. Hennet, I. Pozdnyakova, V. Cristiglio, G. J. Cuello, S. Jahn, S. Krishnan, M.-L. Saboungi and D. L. Price, *J. Phys.: Condens. Matter*, 2007, **19**, 455210.
24 C. Landron, L. Hennet, T. E. Jenkins, G. N. Greaves, J. P. Coutures and A. K. Soper, *Phys. Rev. Lett*., 2001, **86(21)** , 4839.
25 L. Hennet, I. Pozdnyakova, V. Cristiglio, S. Krishnan , A. Bytchkov, F. Albergamo, G.J. Cuello, J.-F. Brun, H.E. Fischer, D. Zanghi, S. Brassamin, M.-L. Saboungi and D.L. Price, *J. Non-Crystalline Solids.*, 2007, **353**, 1705.
26 G. N. Greaves and S. Sen, *Adv. Phys.*, 2007, **56(1)**, 1.
27 M. Wilson and P. A. Madden, *J. Phys.: Condens. Matter*, 1993, **5**, 2687.
28 M. Salanne and P. A. Madden, *Mol. Phys.*, 2011, **109(19)**, 2299.
29 M. Salanne, C. Simon, P. Turq and P. A. Madden, *J. Phys. Chem. B*, 2007, **111**, 4678.
30 V. Sarou-Kanian, A.-L. Rollet, M. Salanne, C. Simon, C. Bessada and P. A. Madden, *Phys. Chem. Chem. Phys.*, 2009, **11**, 11501.
31 C. Merlet, P. A. Madden and M. Salanne, *Phys. Chem. Chem. Phys.,* 2010, **12**, 14109.
32 S. Jahn and P. A. Madden, *J. Non-Crystalline Solids*, 2007, **353**, 3500.
33 S. Jahn and P. A. Madden, *Condens. Matter Phys.*, 2008, **11(1)**, 169.
34 M. Salanne, B. Rotenberg, S. Jahn, R. Vuilleumier, C. Simon and P. A. Madden, *Theor. Chem. Acc*., 2012, **131**, 1143. arXiv:1204.1427.
35 O. Pauvert, M. Salanne, D. Zanghi, C. Simon, S. Reguer, D. Thiaudière, Y. Okamoto, H. Matsuura and C. Bessada, *J. Phys. Chem*., 2011, **115,** 9160.
36 P. A. Madden, K. O'Sullivan, J. A. Board and P. W. Fowler, *J. Chem. Phys.*, 1991, **94**, 918.
37 E. Stefanidaki, G. M. Photiadis, C. G. Kontoyannis, A. F. Vik and T. Østvold, *J. Chem. Soc*., *Dalton Trans*., 2002, 2302.
38 H. Xiao, J. Thonstadt and S. Rosleth, *Acta Chem. Scand*., 1995, **49**, 96.
39 M. H. Brooker, R. W. Berg, J. H. von Barner and N. J. Bjerrum, *Inorg. Chem.*, 2000, **39**, 4725.
40 J. Nakano, *Asia Pac. Bull*., 2012, **163**.
41 J. Uhlir, *J. Nucl. Mater*., 2007, **360**, 6.
42 S. Delpech, C. Cabet, C. Slim and G. S. Picard, *Materials Today*, 2010, **13(12),** 34.
43 P. Taxil, L. Massot, C. Nourry, M. Gibilaro, P. Chamelot and L. Cassayre, *J. Fluorine Chem*., 2009, **130**, 94.
44 P. Chamelot, L. Massot, C. Hamel, C. Nourry and P. Taxil, *J. Nucl. Mater*., 2007, **360**, 64.
45 V. Lacassagne, C. Bessada, B. Ollivier, D. Massiot and J.-P. Coutures, *C. R. Acad. Sci. IIb*, 1997, 91.
46 D. Massiot, F. Fayon, M. Capron, I. King, S. Le Calve, B. Alonso, J. –O. Durand, B. Bujoli, Z. Gan and G. Hoatson, *Magn. Reson. Chem*., 2002, **40**, 70.
47 A. Baranyai, I. Ruff and R. L. McGreevy, *J. Phys. C: Solid State Phys.*, 1986, **19**, 453.
48 M. C. C. Ribeiro, *J. Phys. Chem. B*, 2003, **107**, 4392.
49 M. Mansmann, *Z. Kristallogr.*, 1965, **122**, 375.
50 B. Maximov and H. Schulz, *Acta Crystallogr*., 1985, **41**, 88.
51 A. Zalkin and D. H. Templeton, *Acta Crystallogr*., 1985, **41**, 91.
52 W.H. Zachariasen, *Acta Cryst*., 1951, **4**, 231.
53 T. Petzel, V. Marx and B. Hormann, *J. Alloys Compd.*, 1993, **200**, 27.
54 W. Klemm and H. A. Klein, *Z. Anorg. Allg. Chem.*, 1941, **248**, 167.
55 J. Lee, Q. Zhang and F. Saito, *J. Am. Ceram. Soc.*, 2001, **84(4)**, 863.
56 J. Lee, Q. Zhang and F. Saito, *J. Alloys Compd.*, 2003, **348**, 214.
57 A.-L. Rollet, E. Veron and C. Bessada, *J. Nucl. Mater*., 2012, **429**, 40.
58 D. Kruk, O. Lips, P. Gumann, A. Privalov and F. Fujara, *J. Phys.: Condens. Matter*, 2006, **18**, 1725.

59 A.F. Privalov, I.V. Murin and H.-M. Vieth, *Solid State Ion.*, 1997, **101-103**, 393.
60 V.V. Sinitsyn, O. Lips, A.F. Privalov, F. Fujara and I.V. Murin, *J. Phys. Chem. Solids.*, 2003, **64**, 1201.
61 J. Schoonman, G. Overluizen and K. E. D. Wapenaar, *Solid State Ionics*, 1980, **1**, 211.
62 A. Roos, A. F. Aalders, J. Schoonman, A. F. M. Arts and H. W. De Wijn, *Solid State Ionics*, 1983, **9-10**, 571.
63 N. I. Sorokin, M. V. Fominikh, E. A. Krivandina, Z. I. Zmurov and B. P. Sobolev, *Kristalografiya*, 1996, **41**, 310.
64 C. Hoff, H.-D. Wiemhöfer, O. Glumov and I. V. Murin, *Solid State Ionics*, 1997, **101-103**, 445.
65 J. W. Fergus and H.-P. Chen, *J. Electrochem. Soc.*, 2000, **147(12)**, 4696.
66 K. T. Jacob and V. S. Saji, *Int. J. Appl. Ceram. Technol.*, 2006, **3(4)**, 312.
67 M. Ambrová, J. Juricová, V. Danielik and J. Gabcová, *J. Therm. Anal. Calorim.*, 2008, **91**, 569–573.
68 A.-L. Rollet, A. Rakhmatullin and C. Bessada, *Int. J. thermophys.*, 2005, **26**, 1115.
69 A.-L. Rollet, M. Salanne and H. Groult, *J. Fluorine Chem.*, 2012, **134**, 44.
70 V. Dracopoulos, B. Gilbert, B. Borrensen, G. M. Photiadis, and G. N. Papatheodorou, *J. Chem. Soc. Faraday Trans.*, 1997, **93**, 3081.
71 V. Dracopoulos, J. Vagelatos and G. N. Papatheodorou, *J. Chem. Soc.*, *Dalton Trans.*, 2001, 1117.
72 A.-L. Bieber, L. Massot, M. Gibilaro, L. Cassayre, P. Chamelot and P. Taxil, *Electrochim. Acta*, 2011, **56**, 5022.
73 M. Kergoat, L. Massot, M. Gibilaro and P. Chamelot, *Electrochim. Acta*, 2014, **120**, 258.
74 G. Z. Chen, D. J. Fray and T. W., *Nature*, 2000, **407**, 361.
75 M. Gibilaro, J. Pivato, L. Cassayre, L. Massot, P. Chamelot and P. Taxil, *Electrochim. Acta*, 2011, **56**, 5410.
76 K. J. Ooms, K. W. Feindel, M.J. Willans, R. E. Wasylishen, J. V. Hanna, K. J. Pike and M. E. Smith, *Solid State Nucl. Magn. Reson.*, 2005, **28**, 125.
77 A.-L. Rollet, M. Allix, E. Veron, M. Deschamps, V. Montouillout, M. R. Suchomel, E. Suard, M. Barre, M. Ocaña,∇A. Sadoc, F. Boucher, C. Bessada, D. Massiot and F. Fayon, *Inorg. Chem.*, 2012, **51**, 2272.
78 R. Dupree, M. H. Lewis and M. E. Smith, *J. Am. Chem. Soc.*, 1989, **111**, 5125.
79 T.J. Bastow, T. Mathews and J.R. Sellar, *Solid State Ionics*, 2004, **175**, 129.
80 L. Spencer, E. Coomes, E. Ye, V. Terskikh, A. Ramzy, V. Thangadurai and G. R. Goward, *Can. J. Chem.*, 2011, **89**, 1105.
81 P. P. Fedorov, *Russ. J. Inorg. Chem*, 1999, **44(11)**, 1703.
82 M. Beilmann, O. Beneš, R. J. M. Konings and T. Fanghänel, *J. Chem. Thermodyn.*, 2011, **43**, 1515.
83 F. Abdoun, M. Gaune-Escard and G. Hatem, *J. Phase Equilib.*, 1997, **18**, 6.
84 J. P. M. van der Meer, R. J. M. Konings, K. Hack and H. A. J. Oonk, *Chem. Mater.*, 2006, **18**, 510.
85 A. I. Agulyanskii and V. A. Bessonova, *Zh. Neorg. Khim.*, 1982, **27 [4]**, 1029-1032; *Russ. J. Inorg. Chem.* (Engl. Transl.), 1982, **27 [4]** 579.

In-situ high temperature NMR technique evidences the local structure of lithium lanthanum oxyfluoride melts.